



LAWRENCE
LIVERMORE
NATIONAL
LABORATORY

Increasing robustness of indirect drive capsule designs against short wavelength hydrodynamic instabilities

S. W. Haan, M. C. Herrmann, T. R. Dittrich, A. J. Fetterman, M. M. Marinak, D. Munro, S. M. Pollaine, J. D. Salmonson, G. L. Strobel, L. J. Suter

December 6, 2004

Physics of Plasmas

Disclaimer

This document was prepared as an account of work sponsored by an agency of the United States Government. Neither the United States Government nor the University of California nor any of their employees, makes any warranty, express or implied, or assumes any legal liability or responsibility for the accuracy, completeness, or usefulness of any information, apparatus, product, or process disclosed, or represents that its use would not infringe privately owned rights. Reference herein to any specific commercial product, process, or service by trade name, trademark, manufacturer, or otherwise, does not necessarily constitute or imply its endorsement, recommendation, or favoring by the United States Government or the University of California. The views and opinions of authors expressed herein do not necessarily state or reflect those of the United States Government or the University of California, and shall not be used for advertising or product endorsement purposes.

Increasing robustness of indirect drive capsule designs against short wavelength hydrodynamic instabilities

Steven W. Haan, Mark C. Herrmann, Thomas R. Dittrich, Abraham Fetterman, Michael M. Marinak, D. Munro, Stephen M. Pollaine, Jay D. Salmonson, George L. Strobel, and Laurence J. Suter

Lawrence Livermore National Laboratory
Livermore, CA 94550

Target designs are described that are meant to achieve ignition on the National Ignition Facility. Simulations of recent indirect drive cryogenic capsule designs indicate dramatically reduced growth of short wavelength hydrodynamic instabilities, resulting from two changes in the designs. First, better optimization results from systematic mapping of the ignition target performance over the parameter space of ablator and DT-ice thickness combinations, using techniques developed by one of us (Herrmann). After the space is mapped with one-dimensional simulations, exploration of it with two-dimensional simulations quantifies the dependence of instability growth on target dimensions. Low modes and high modes grow differently in different regions of the space, allowing a trade-off of the two regimes of growth. Significant improvement in high-mode stability can be achieved, relative to previous designs, with only insignificant increase in low-mode growth. This procedure produces capsule designs that, in simulations, tolerate several times the surface roughness that could be tolerated by capsules optimized by older more heuristic techniques. Another significant reduction in instability growth, by another factor of several, is achieved with ablators with "graded dopants." In this type of capsule the mid-Z dopant, which is needed in the ablator to minimize x-ray preheat at the ablator-ice interface, is optimally positioned within the ablator. A fabrication scenario for graded dopants already exists, using sputter coating to fabricate the ablator shell. We describe the systematics of these advances in capsule design, discuss the basis behind their improved performance, and summarize how this is affecting our plans for NIF ignition.

This work was performed under the auspices of the U.S. Department of Energy by the University of California, Lawrence Livermore National Laboratory under contract No. W-7405-Eng-48.

Note to referee and editor: I am sorry that the figures and references are in such sad shape, please forgive me. I intend to prepare publication quality figures before the next iteration. I regard only Figs. 1, 2, and possibly 9 as ready to go. I am not intending significant changes in the figure content, and I would appreciate any comments you have on the content (especially any comments on how I should try to change Fig. 10 would be useful...) Of course I will get all the references in place.

INTRODUCTION

A number of target designs have been proposed to produce thermonuclear ignition on the National Ignition Facility (NIF) [1]. New targets are described here that are substantially less unstable hydrodynamically than previous designs. These targets, Fig. 1, use *indirect drive*: the laser heats the interior of a gold cylinder, a *hohlraum*, to very high temperature (250-300 eV) [2]. The x-rays filling the hohlraum ablate the outside of the spherical fuel capsule at its center, imploding and compressing deuterium-tritium (D-T) fuel. The fuel is initially in a spherical shell of solid D-T held at cryogenic temperature before the shot, self-smoothed by β -particle deposition from the T decay [3]. The laser pulse, Fig. 2, is tuned to launch four shocks and implode the capsule with the fuel close to Fermi-degenerate. This basic configuration has been the same since indirect drive ignition was first proposed for the NIF; the innovations described here pertain to the optimization of the ablator characteristics, both its dimensions and composition, and the layers of Cu dopant in the ablator as they determine the hydrodynamic instability growth.

Several substances have been proposed for the ablator. Its material properties, primarily its opacity, control the hydrodynamic instability that can disrupt the implosion. (There is a substantial literature on these instabilities, reviewed in ref. [2].) The instability growth determines specifications for roughness on the ablator and the D-T ice. Whether these specifications can plausibly be met determines the viability of a target; this and laser-plasma instabilities are the controlling features determining the size of the NIF facility.

The work described herein indicates that the use of radially graded Cu dopant in Be confers remarkable stability on capsules for NIF, allowing them to tolerate surfaces 20 times rougher than typical first-generation NIF targets. With detailed optimization, uniformly doped Be(Cu) targets can also perform much better than the original designs—in this case about 8 times rougher. This qualitative change in stability can allow for either significantly rougher surfaces than previously specified, or for reconfiguration of the target to accommodate other changes in the design. It probably relaxes the size requirement on tubes that could be used to fill capsules, making more feasible a fielding scenario in which the

capsules are filled through a tube rather than being diffusion filled as originally proposed. This could allow for significant simplification of the cryogenic fielding hardware, since diffusion-filled capsules typically cannot hold the pressure at room temperature and must be kept cold once filled.

The first capsules considered for NIF assumed an ablator made of Be doped with ~1% Na and Br, radially varying within the shell. One such design, at 250 eV peak drive, is described in ref. [2]. These early designs used a less optimal grading scheme than described herein. The original Be(graded Na-Br) designs were supplanted in the planning and design by plastic capsules doped uniformly with Br, CH(Br) [4]. At that time it was believed that fabrication and fielding would be easiest with uniformly doped CH(Br). Targets were subsequently proposed with ablators of uniformly Cu doped Be [5], and of undoped polyimide [6]. Be is doped with Cu since it is known that Cu dissolves atomically in solid Be at the relevant concentrations of ~1%; the choice of dopant material is not tightly constrained, provided that the dopant increases the opacity to hard x-rays while minimally increasing the opacity for the bulk of the x-rays in the drive. CH capsules can be doped with either Br or Ge. Polyimide, with its O and N content, is best left undoped at 300 eV, and is too opaque to make a good ablator at 250 eV. These three ablators—polyimide, CH(Ge), and Be(Cu), all uniformly doped or undoped—have been the mainline NIF targets, and considerable work has been done investigating their features [6,7,8,9]. Concurrently, some work was done with radially graded dopants. Dittrich [10] described a 250 eV Be(graded Cu) design, implementing a scheme attributed to Hatchett (unpublished) and considered in more detail below. Another graded dopant approach, with a layer of clean Be inside of an otherwise uniformly doped Be(Cu) shell, was considered in a 350 eV Be(Cu) design by Hinkel [11].

All the early targets were heuristically optimized: the designers used guidelines based on two dimensional simulations and physical principles to optimize a design in one dimension, and its properties were explored in 2D and 3D. The scans used for optimization were expanded to scans over one parameter, [10] and then the two parameters of ablator and fuel thickness [12]. As described in more detail below, the optimization process was automated by one of us (Herrmann) allowing for much more detailed scans over the parameter spaces of possible designs. Given these detailed scans, more systematic 2D optimization is also possible. That process is described below and then used to consider the impact of varying dopant concentration, for uniformly doped Be(Cu) targets.

Once the uniformly doped targets have been fully optimized, the next possibility to consider is spatially varying the dopant. One such design from Ref. [10] was meant to explore the limits of extremely small size and low temperature, to see whether such a design might feasibly work. Hence it very small, and driven at low temperature (250 eV). That work

concluded that the capsule was too marginal to be feasible as a proposed design. Larger scales of Dittrich's design were not considered at that time. Subsequently, Strobel et al. [12,13] and Bradley et al. [14] found that uniformly doped 250 eV Be(Cu) designs using more typical NIF power and energy. They found that, in order to be comparable to the Dittrich design in margin against hydrodynamic instability growth, the uniformly doped targets required considerably more power and energy than the Dittrich design. This suggested that the Hatchett-Dittrich doping scheme conferred more stability than originally recognized. Haan's original 250 eV design [2], with graded dopant but less well optimized, was intermediate in stability (the three designs are compared in ref.13). In this paper, the Dittrich design is examined at scales comparable to those considered in refs. [12-14], and is found to be substantially more stable. The same graded-dopant scheme is also implemented in a 300 eV design, at a baseline power-energy scale, and it is also much more stable than any other design at comparable power and energy.

Many of the fabrication considerations that led to preference of CH over Be(Cu) have changed so that Be is now considered very attractive for fabrication. One consideration, the possible roughness of the surface, is addressed directly by the design concepts described here, since these designs can tolerate significantly rougher surfaces. Characterization of the ice layer inside of the optically opaque Be has been demonstrated using x-ray refractive imaging [15,16]. CH had been considered advantageous because it leaves open the possibility of smoothing the layer with infrared deposition, but the layers seen inside of Be with only β energy deposition appear to be adequate, especially given the reduced stability requirement with graded dopant. Finally, diffusion fill had been thought to be advantageous since it eliminated a fill tube, and it was thought that Be could not be diffusion filled. However, the fielding simplifications resulting from the use of a fill tube are now thought to be more important than the deleterious impact of the tube. Fabricating the layers of varying Cu concentration is a straightforward extension of technology already being developed for Be ablaters, using sputtering coating: the Cu concentration can be varied in time as the coating is deposited.

The remainder of this paper is as follows. Section II has details of the simulation techniques. Sections III, IV, and V describe the Be(Cu) designs we are considering here; Section VI compares these targets via 2D simulations. Section VII is a conclusion.

II. SIMULATION DETAILS

The simulations described here were done with the codes Lasnex [17] and Hydra [18]. One-dimensional simulations were done with full multi-group radiation transport, and with multi-group radiation diffusion. The diffusion simulations use a mean-free-path-to-boundary scheme and few-group weighted opacities, and have the drive spectrum adjusted

slightly to make them more closely match the simulations with full transport. They reproduce highly resolved 1D multi-group transport simulations to about 1% in all of ablation rate, implosion history, and density profiles. Two-dimensional simulations used to evaluate the hydrodynamic instability growth use the same diffusion setup. They have been done with XSN opacities [19], and with opacity tables generated [20] using the Opal [21] model for the low atomic number ions and the STA [22] model for the Cu. The two opacity models give essentially identical results. Most of the simulations have been done with QEOS equation of state [23], with parameters set so that the DT EOS is intermediate within the range seen in recent experiments [24-26]. The simulations use a frequency-dependent source, with a spectrum extracted from gold hohlraum simulations. The M-band content in the spectrum is similar to that described in ref. 12.

There are two ways to simulate the growth and impact of hydrodynamic instability growth. Single modes can be initialized with small amplitudes so that they stay linear throughout the implosion. These are used to evaluate the amount of instability growth for each individual perturbation. To simulate the net impact of the instability growth it is necessary to do simulations that include a wide spectrum of modes, with realistic initial amplitudes. Such simulations have been done for the capsules described here, using the spectrum of initial perturbations described in ref. [10]. When the rms is 10 nm, this spectrum corresponds to the high-mode part of the “NIF standard” spectrum used by the target fabrication community as a roughness goal [27]. Various surface roughnesses are modeled by multiplying the perturbation by an overall multiplier. Only modes 12 and above are typically included in these simulations (lower modes can be included in other simulations as described below).

III. OPTIMIZATION OF UNIFORMLY DOPED Be(Cu) DESIGN

A new way to provide the optimization of capsules has been developed by one of us (Mark Herrmann). Herrmann's innovations have been a better implementation of the constraints than previously, and an automated process that thoroughly optimizes over the remaining free parameters. Ultimately the true constraints are on hohlraum size, as that determines the hohlraum energetics, and on the temperature vs. time profile as determined by the laser power and energy. These in turn constrain (i) the capsule size, as that affects case-to-capsule ratio, (ii) the peak temperature T_R , and (iii) to a good approximation, the time integral of $T_R^4(t)$. This set of constraints is slightly different from past work, where we considered the absorbed energy as being the primary quantity to hold fixed. Herrmann argues that capsules with lower albedos, which can absorb more energy at given size and T_R , should not be "punished" for this better performance. Thus the capsule absorbed energy is not constrained in the optimization, although of course it does not vary very much for a given material, given the constraints on outer radius, peak T_R , and integral of $T_R^4(t)$.

After we fix these three parameters, a capsule design is characterized by ablator material, ablator thickness, fuel thickness, and the detailed shape of $T_R(t)$. For a given ablator material, and assuming that we can optimize $T_R(t)$, that leaves a two-dimensional parameter space of fuel thickness and ablator thickness. At each point in this space, Herrmann's scheme automatically adjusts the drive profile using a set of scripts running LASNEX and adjusting the profile to produce the shock timing determined to optimal by Munro [28]. A scan over the thicknesses then provides a map of yield in the two dimensional parameter space of shell thicknesses, as shown by the yield contours in Fig. 3. When the ablator is too thin, it burns through and the target fails to ignite. When the shells are too thick, the velocity is inadequate and again the target fails. In between is the operating space.

This procedure is the maturation of an approach described by Dittrich [5,10], who did scans over ablator thickness at constant fuel mass, and by Strobel [12] who did a 2D scan over ablator and fuel thickness similar to what Herrmann has done. Dittrich and Strobel both tuned the individual designs by hand, so the scans were necessarily less complete and more noisy, and they kept absorbed energy fixed rather than outer radius. All of the results have given very similar results; the modern technique allows for more accurate and complete scans, and more of them.

Having defined the space of one-dimensional performance, we can then explore the 2D (and presumably 3D) characteristics. As shown in Fig. 3, short-wavelength Rayleigh-Taylor is generally worse as we move towards thinner shells within this space. Sensitivities to longer wavelength target fab defects, or to asymmetry, depend more on deceleration Rayleigh-Taylor and accordingly are worse for the lower velocity targets with thicker shells. Because the short-wavelength Rayleigh-Taylor has more e-foldings of growth, it is generally more sensitive, i.e. the overall optimization tends to be more influenced by the short wavelengths than the long, pushing us towards thicker shells than previously thought optimal. Once the implosion velocity is above about $37 \text{ cm}/\mu\text{s}$ (at 1.11 mm outer radius for plastic capsules) the long wavelength robustness does not increase very much with velocity, so the optimum design is probably that which has velocity just at $37 \text{ cm}/\mu\text{s}$. While this specific optimization is valuable, the most important product of this work is a quantification of the tradeoff, and the creation of the tools to evaluate the whole space of targets. Future work will change the specifics, and tell us which source of perturbation is dominant; now we have the tools to evaluate the relative importance of future results.

This scan technique has been applied to a variety of targets, including: the CH(Br) "scale 1" 300 eV capsule shown in Fig. 2; polyimide at the same outer radius and peak drive; Be(Cu) under the same conditions, as described in more detail below; and three ablator materials at 250 eV: CH(undoped), polyimide, and Be(Cu). We find that at 250eV,

undoped CH has similar yield to uniformly doped Be(Cu), and can tolerate similar surface roughness (about 75 nm in spherical harmonic modes above 10, assuming a standard surface power spectrum, at a scale where the capsule absorbs 350 kJ). At this low drive temperature, both are considerably superior to polyimide, which gives similar yield but requires the ablator surface to be a factor of several smoother.

We have done this optimization for Be(Cu) designs at various Cu concentrations. At lower Cu levels the targets optimize with thicker ablators, as expected. All targets had 1110 μm outer radius, 0.3 mg/cc DT gas density, and a source corresponding to 1.4 MJ of laser energy absorbed by a standard gold hohlraum. We then selected a similarly optimized design at each of several Cu concentrations: 0.4%, with dimensions 175x80; 0.7%, 158x80; 0.9%, 150x80; 1.1%, 145x80; and 1.5%, 133x80. In addition to having the same fuel thickness, these all have the same implosion velocity of 3.7×10^7 cm/s. Yields are all very close to 20 MJ. More details about these designs will be presented below, in comparison with the graded doped designs.

IV. 5 layer graded doped designs

When Strobel et al. did an optimization of 250 eV Be(Cu) capsules, similar to that described above although less complete, they found that their optimized 250 eV target at 190 kJ was not much more robust than a 5-layer graded doped design published by Dittrich [10] that only absorbed 95 kJ. That suggested that graded doped capsules were superior to uniformly doped capsules, although they had never been compared in detail. (Strobel's optimization, while crude, has been confirmed by application of the technique described above.) The design in Ref. 10 was very small, intended to probe the limits of what capsules may ignite on NIF. Dittrich did not consider larger scales. We have now found that when the target is taken to larger scales it is remarkably less sensitive to ablator roughness than are the uniformly doped Be(Cu) capsules. This comparison is shown in Fig. 5.

A design at 300 eV was based on Dittrich's design: the thicknesses are essentially the same as the appropriate scale of the 250 eV design, but the radius was decreased and the dopant level increased. This results in a 300 eV design, shown in Fig. 1, the features of which are described in more detail below.

IV. 2 layer graded dopant design

The two desirable features of a graded doped design are (i) a low dopant on the outside, to minimize instability growth during acceleration; and (ii) an undoped region immediately next to the fuel which does not preheat, hence staying at higher density and reducing instability growth at the fuel/ablator interface. The simplest way to achieve this is to take a low-level doped design — we used the 0.4% design described above — and replace some of the inner ablator

with undoped Be. The appropriate amount of clean Be can be seen by varying the thickness of the clean layer, as shown in Fig. 6. If the undoped layer is too thick, it begins to ablate and the material next to the fuel is no longer protected from preheat. The density next to the fuel is maximized for a clean thickness of about 5 μm . This defines our 2-layer design: the same as the 0.4% design optimized above, but with the inner 5 μm of Be undoped.

Neither graded doped capsule has yet been systematically optimized; doing so may or may not improve performance beyond the heuristically optimized current design. Dittrich's original small scale 250 eV graded doped design was optimized with a moderately systematic approach, not quite as elaborate as modern techniques allow.

Note that the uniformly doped targets, and the 2-layer graded dopant, have outer radius 1110 μm while the 5-layer design is 1105 μm . This small inequivalence, a historical artifact, could have resulted in a few percent increase in the specifications for the larger targets.

V. Comparison of designs via 2D simulations

The in-flight density profiles for the 5 capsules considered here are shown in Fig. 7. The uniformly doped capsules show the expected dependence on dopant: more highly doped capsules have a steep, unstable ablation front, while the most lightly doped capsules are more stable there but have a large density step at the outside of the fuel. The 2-layer design has the desired high density region just outside the fuel, while the 5 layer design has both the high density region and the best ablation front features.

The most direct way to compare the stability of the designs is with multi-mode 2D simulations that vary the initial amplitude. The result of doing so is shown in Fig. 8 for the three uniformly doped targets. By this way of evaluating the growth, the 0.4% target is the most robust. However, this target has substantial short wavelength growth as described below.

A similar plot for the graded doped designs is in Fig. 9. They are much more stable. The 5-layer design is somewhat more stable than the 2-layer design, although the latter is quite a bit better than any of the uniformly doped designs from Fig. 8.

The stability of these targets does not appear to be a result of fine optimization of the dopant profile. As evidence for that, Figs. 9 shows 2D simulations of a design in which the inner two steps of the dopant profile from the 5-layer design are replaced with a constant dopant concentration at the highest level of 0.7%. This increases the instability growth only slightly. From a functional optimization point of view, it appears that the optimum is fairly broad; if the dopant is not constrained to be uniform, there is a wide variety of profiles that give performance better than any uniform dopant level.

The other way to examine the growth of perturbations is to do simulations of one mode at a time. These are easier to validate, and can be easier to understand. Growth factor calculations are shown in Fig. 10. Note that there is significant short wavelength growth for all cases, but especially for the 0.4% uniformly doped capsule.

Provided the initial surface roughness is smooth enough that the capsule survives past peak velocity, the other growth that is important is to the hot-spot perimeter at ignition time, Fig. 10b. Note that the modes with the most hot-spot growth, around 20, have about 75% more growth in the uniformly doped capsule, and about the same proportion for these modes for the growth on the outside. This is about the same difference as seen for these two capsules in Fig. 10a, indicating that the reduced growth from ablation stabilization, from these intermediate modes, is what ultimately matters. At higher modes, where the most dramatic difference is evident in Fig. 10a, the growth does not couple through to the hot-spot and is small for both capsules. In the actual experiment these high modes may or may not matter, depending on the spectrum of initial perturbations, as they determine whether the shell survives past peak velocity. The high modes might be more important to the growth of perturbations seeded by a fill tube, which is initially at very high mode number. Fill tube simulations are in progress for both the uniform and the graded doped capsules.

Ice roughness perturbations have been studied only very slightly at the time of this writing, but indication is that the graded doped capsules can also tolerate ice roughness a factor of several larger than typical previous capsules. (Note to referee: I will probably be able to amplify on this in the next version. Also, either John Edwards – the following paper – or I will probably include a figure showing how the fill tube requirement is likely to be relaxed by using a graded dopant.)

VI. Conclusion

The original NIF targets required surface roughness of 10-30 nm. By systematic reoptimization, we have increased the tolerable surface roughness for CH(Ge) capsules to 65 nm, and for uniformly doped Be(Cu) targets to 150 nm. The specifications for surface roughness must leave margin for other sources of error, and these numbers are the ablator roughness at which it alone degrades the yield. Hence the specification is about 1/3 of the numbers given here. A detailed rollup of all of the sources of uncertainty, for the new targets, is being developed for future publication. By using graded dopant in the Be, we find that the capsule can tolerate a roughness of 600 nm (again, for roughness alone).

[1] J. A. Paisner et al., Laser Focus World 30, 75 (1994).

[2] J. D. Lindl, Inertial Confinement Fusion (Springer-Verlag, New York, 1998).

- [3] beta layering, need to update reference
- [4] S. W. Haan et al., *Physics of Plasmas* 2, 2480 (1995).
- [5] D. C. Wilson et al., *Physics of Plasmas* 5, 1953 (1998)
- [5] Dittrich T.R. *et al.* 1999 *Phys. Plasmas* 6 2164 (make sure this is polyimide first publication)
- [6] Marinak M.M. *et al.* 1998 *Phys. Plasmas* 5 1125
- [7] Dittrich, target fab update
- [8] Krauser et al. *Phys. Plasmas* 1997 (need to get reference)
- [9] (robustness study, need to get reference)
- [10] Dittrich T.R. *et al.* 1998 *Phys. Plasmas* 5 3708
- [11] Hinkel D.E. *et al.* 2004 *Phys. Plasmas* 11 1128
- [12] Strobel G.L. *et al.* 2004 *Phys. Plasmas* 11, 1617
- [13] Strobel, G.L. *et al.* 2004 *Phys. Plasmas*, scaling
- [14] Bradley P.A. and Wilson D.C. 1999 *Phys. Plasmas* 6 4293
- [15] Montgomery, x-ray refractive imaging
- [16] Koziolowski, x-ray refractive imaging
- [17] Zimmerman G. and Kruer W.L. 1975 *Comments Plasma Phys. Controlled Fusion* 2 85
- [18] Hydra
- [19] XSN
- [20] John Castor, private communication
- [21] Opal
- [22] STA
- [23] qeos
- [24] nova DT eos
- [25] Z DT eos
- [26] other recent DT eos, may have to be private communication
- [27] Bob Cook, publication of NIF standard surface roughness
- [28] Munro, *Phys Plasmas*, shock timing

Fig. 1. Target proposed to achieve ignition on the National Ignition Facility. (a) Hohlräum (b) Capsule with 5-layer graded doped beryllium ablator.

Fig. 2. Laser power to drive the target, and the corresponding temperature vs time in the hohlraum. This baseline target uses 1.4 MJ of 0.3 μm light, at peak power 410 TW. The capsule absorbs 180 kJ, and produces 19 MJ of fusion energy.

Fig. 3. Capsule yield vs. thickness of ablator and fuel. At each set of dimensions the pulse-shape driving the capsule is optimized by an automated routine. The outer radius is held fixed at 1.110 mm, the peak T_R at 300 eV, and the integral of $T_R^4(t)$ is held fixed at a scale corresponding to 1.4 MJ of laser energy. (a) The numbers overlaying the contours indicate the ablator roughness in modes 36-156 that degrades the yield by 50% relative to no roughness. In (b) the numbers indicate the roughness in modes 6-36 that causes 50% yield reduction. Two velocity contours are indicated, in cm/s. In (c) the net roughness requirement is shown. It assumes that the roughnesses as describe in (a) and (b) combine in quadrature; the validity of using the quadrature sum was checked for the central point with lowest roughness requirement.

Fig. 4. Scans over ablator and fuel thickness for two extremes in Cu concentration: (a) 0.4% and (b) 1.5%. Similar scans were done for 0.7%, 0.9%, and 1.1%, with features intermediate between those shown here. The points indicated with black dots are the designs selected for 2D comparison.

Fig. 5. For 250 eV Be(Cu) designs, the ablator roughness requirement vs. capsule absorbed energy. The upper curve is for scales of the original Dittrich graded dopant design, similar to that shown in Fig. 1, and the lower curve is for an optimized uniformly doped design.

Fig. 6. Density vs radius, in flight, for a series of designs with varying thickness of clean beryllium inside of 0.4% Be(Cu). All targets are 175 μm total Be thickness, and had the same drive.

Fig. 7. Density vs radius, in-flight, for graded and uniformly doped Be(Cu) capsules

Fig. 8. Yield vs roughness for the three uniformly doped designs. These simulations include modes above 12, and assume the same power spectrum for the perturbations, described in the text.

Fig. 9. Yield vs. roughness for graded doped capsule designs. The capsules are all “scale 1,” requiring about 1.5 MJ of laser energy absorbed in a 300 eV hohlraum. Solid curves are different designs, at central gas 0.3 mg/cm^3 , and dashed curves show variants on the design from Fig. 1. (a) plastic capsule prior to 2003; (b) recent reoptimization, uniformly 0.7% doped beryllium; (c) graded doped beryllium, per Fig. 1; (d) the 2-layer design; (e) same as c, central gas DT 0.5 mg/cm^3 ; (f) same as (e), with $?? \text{ mg/cm}^3 \text{ } ^3\text{He}$ also included; (g) same as c, but inner two steps of grading replaced with uniform 0.7% Cu.

Fig. 10. Growth factors vs mode number from linear-regime 2D simulations. Solid curves are graded doped capsule, dashed uniformly doped. Curves (a) are amplitude on interface at peak velocity divided by initial amplitude on outside of Be. Curves (b) are growth to perimeter of hot spot at ignition, i.e. 1% burn rate contour when central temperature is 12 keV.

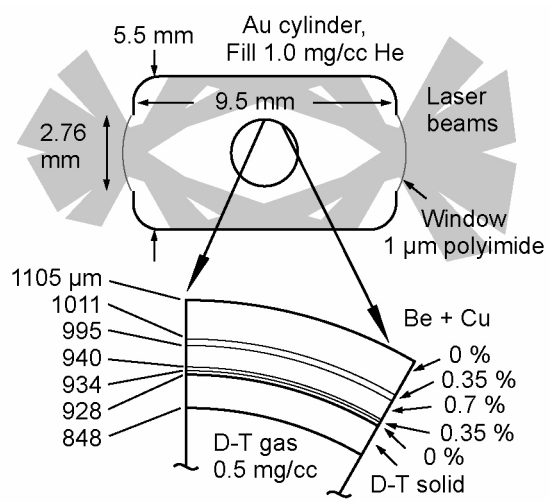


Fig. 1

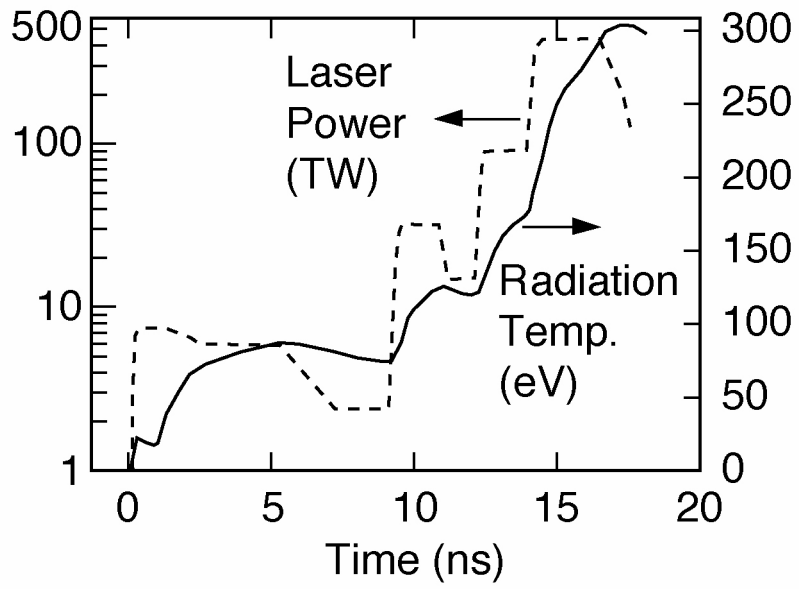


Fig. 2

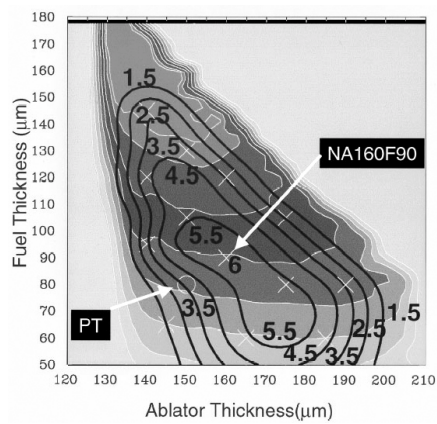
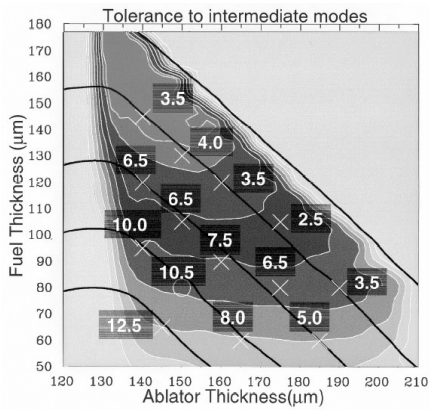
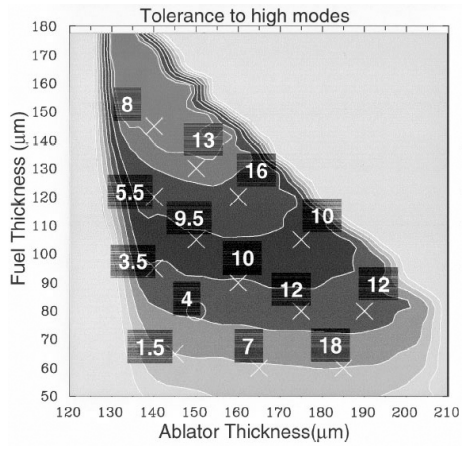


Fig. 3

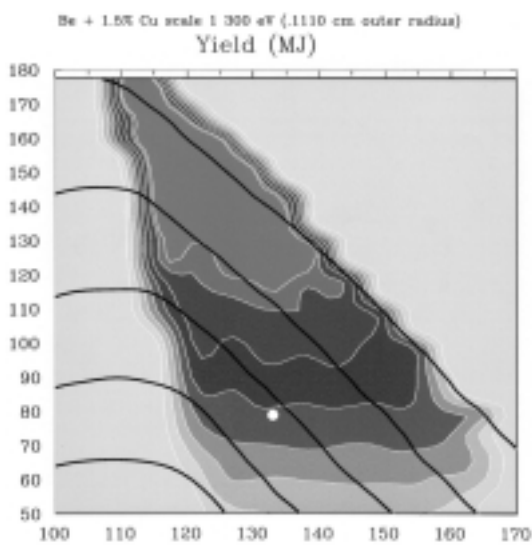
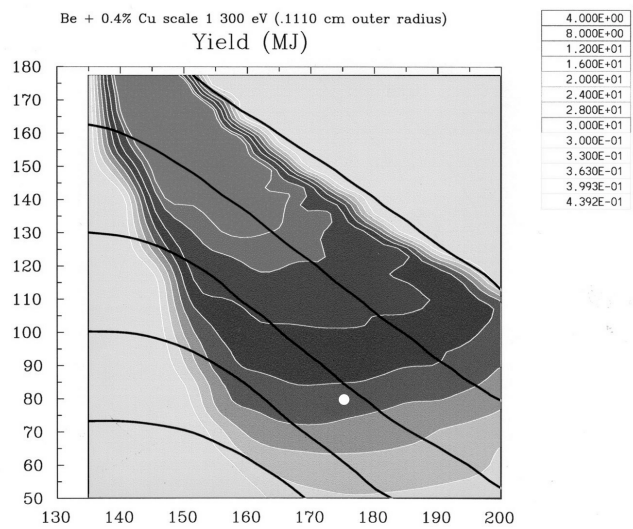


Fig. 4

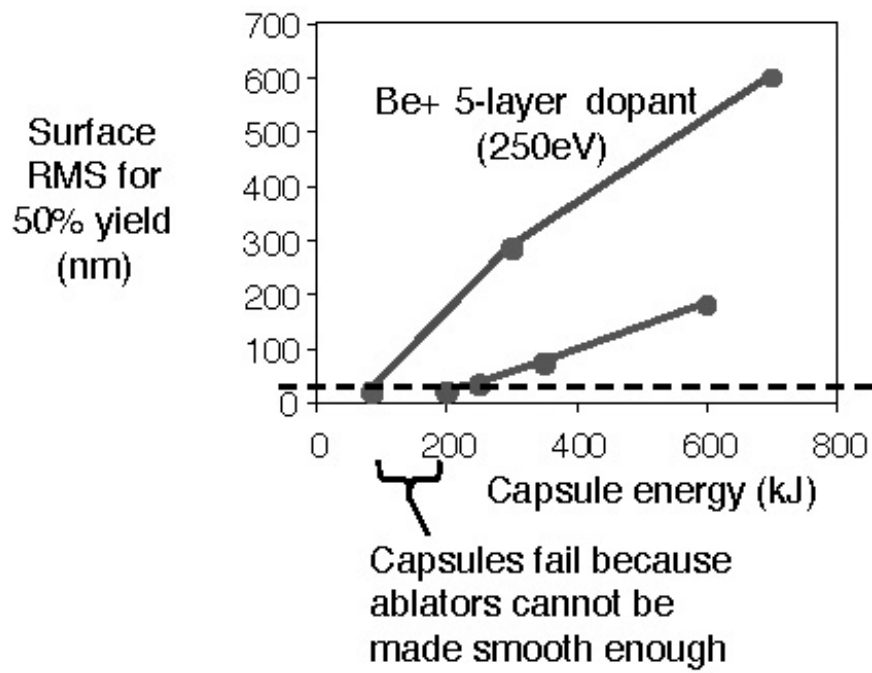


Fig. 5

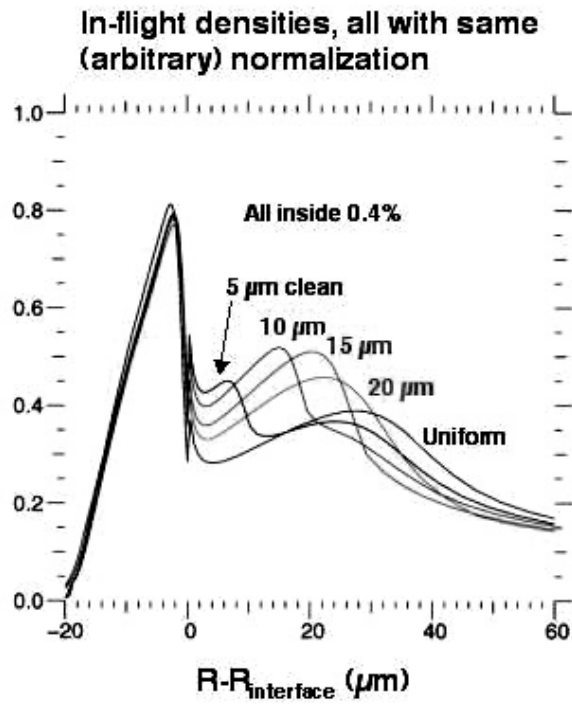


Fig. 6

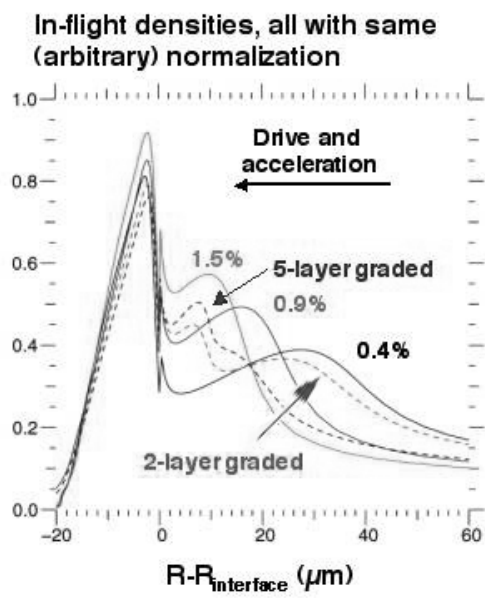


Fig. 7

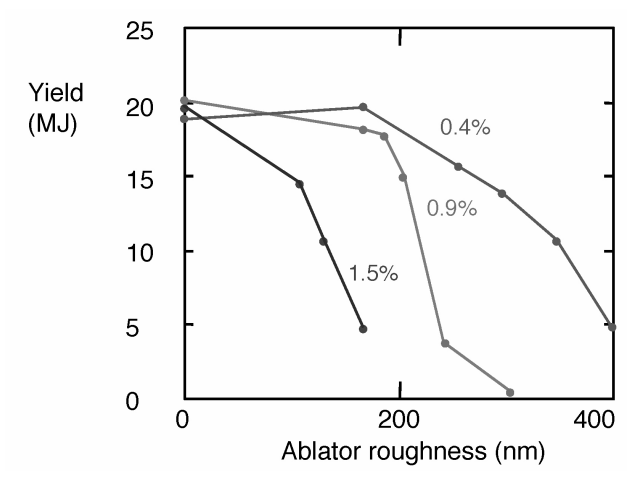


Fig. 8

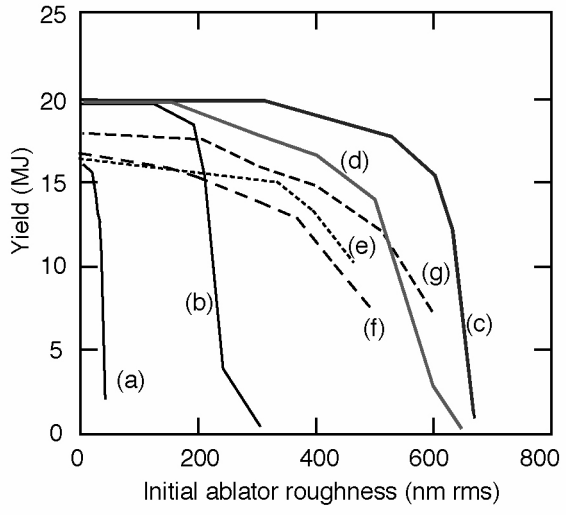


Fig. 9

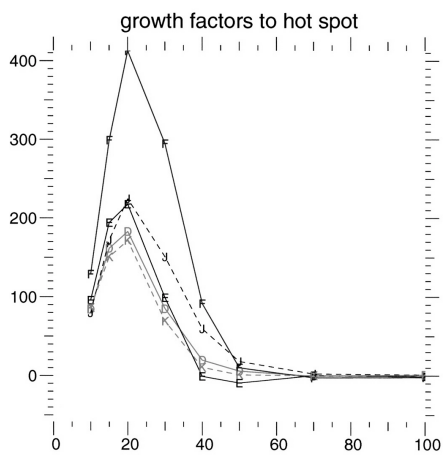
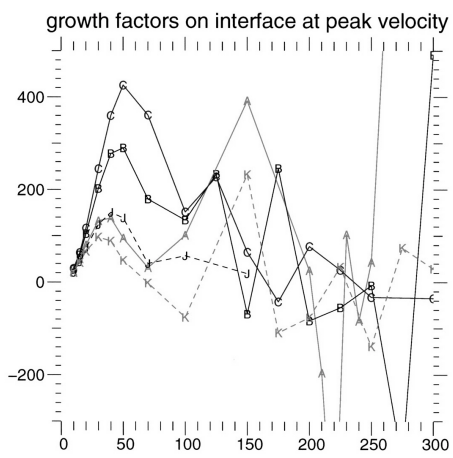


Fig. 10